Journal of Magnetism and Magnetic Materials 427 (2017) 320–324

Contents lists available at ScienceDirect

Journal of Magnetism and Magnetic Materials

journal homepage: www.elsevier.com/locate/jmmm

Particle size- and concentration-dependent separation of magnetic nanoparticles

Kerstin Witte[a,b,*], Knut Müller[b], Cordula Grüttner[b], Fritz Westphal[b], Christer Johansson[c]

[a] University of Rostock, Institute of Physics, Albert-Einstein-Str. 23, 18059 Rostock, Germany
[b] Micromod Partikeltechnologie GmbH, Friedrich-Barnewitz-Str. 4, 18119 Rostock, Germany
[c] Acreo Swedish ICT AB, 40014 Göteborg, Sweden

ARTICLE INFO

Keywords:
Magnetic nanoparticles
Magnetic separation
Magnetic fractionation

ABSTRACT

Small magnetic nanoparticles with a narrow size distribution are of great interest for several biomedical applications. When the size of the particles decreases, the magnetic moment of the particles decreases. This leads to a significant increase in the separation time by several orders of magnitude. Therefore, in the present study the separation processes of bionized nanoferrites (BNF) with different sizes and concentrations were investigated with the commercial Sepmag Q system. It was found that an increasing initial particle concentration leads to a reduction of the separation time for large nanoparticles due to the higher probability of building chains. Small nanoparticles showed exactly the opposite behavior with rising particle concentration up to 0.1 mg(Fe)/ml. For higher iron concentrations the separation time remains constant and the measured Z-average decreases in the supernatant at same time intervals. At half separation time a high yield with decreasing hydrodynamic diameter of particles can be obtained using higher initial particle concentrations.

1. Introduction

Magnetic nanoparticles offer a broad range of potential applications in biomedicine due to their unique chemical and physical properties [1–6]. The particles can be used for magnetic hyperthermia, magnetic resonance contrast imaging, magnetic particle imaging, biosensors, drug delivery and magnetic separation processes. In the latter applications, the particles are used as a carrier to deliver or separate nonmagnetic molecules [7]. While the magnetic separation of targets bound to the particles is obvious, magnetic separation processes are also widely used in the particle synthesis [8].

Magnetophoresis describes the motion of magnetic nanoparticles in a magnetic gradient field considering mainly two different types of particle transport, the cooperative and the non-cooperative magnetophoresis [9]. Cooperative magnetophoresis refers to a fast separation process which is enhanced by particle-particle interactions building particle chains while non-cooperative magnetophoresis is a rather slow process which is characteristic for the motion of single non-interacting particles [9]. In general the separation processes depend on a large number of parameters including the particle size, particle size distribution, surface coating, surface potential, magnetic moment as well as on the particle concentration.

A magnetic separation can be simply achieved by placing a permanent magnet close to a suspension containing magnetic nanoparticles. Using Horizontal Low Gradient Magnetic Field (HLGMF) systems, high magnetic forces, implying fast separation and low magnetic nanoparticle losses can be achieved [10–12]. The magnetophoresis process at HLGMF was discussed to be driven by a cooperative phenomenon consisting of reversible aggregation of particles or chain formation and the movement of the aggregates towards the magnet [10,13]. Due to the magnetic field from the permanent magnets the nanoparticles are magnetized. Together with the field gradient, a magnetic force on the magnetic nanoparticles is created and a drag force is built with opposite orientation when the nanoparticles are moving [7,9].

When the size of the particles decreases, the magnetic moment of the particles reduces [7]. Consequently, the time of the separation process of the particles increases which makes them unattractive for biomedical separation processes. Nevertheless, these particles are of a great interest for other applications like hyperthermia, magnetic resonance, magnetic biodetection as well as magnetic particle imaging.

In terms of quality control it is important to investigate the separation process as a part of the fractionation process after synthesis in order to control the overall distributions of the particle size and of the magnetic particle moment. Therefore, in the present study the magnetophoresis of bionized nanoferrite (BNF) nanoparticles [1] was

* Corresponding author at: University of Rostock, Institute of Physics, Albert-Einstein-Str. 23, 18059 Rostock, Germany.
E-mail address: witte@micromod.de (K. Witte).

http://dx.doi.org/10.1016/j.jmmm.2016.11.006
Received 26 June 2016; Received in revised form 20 October 2016; Accepted 1 November 2016
Available online 03 November 2016
0304-8853/

investigated for a broad range of particle sizes and particle concentrations to demonstrate the analytical and preparative potential of a commercial separator system with a well-defined geometry and field gradients, the Sepmag Q 100 ml (Sepmag Technologies, www.sepmag.eu).

2. Materials and methods

The BNF nanoparticles are multicore particles consisting of individual non-stoichiometric magnetite nanocrystals with cubic or rhombohedral shape with a characteristic individual core size of 10–20 nm covered with a stabilizing starch shell [14,15]. Due to the fact that the nanoparticles are thermally blocked, the dispersed nanoparticles undergo Brownian relaxation meaning that the effective particle magnetic moment is locked to the nanoparticle and rotates with same rate as the particle itself.

All BNF-Starch particles were prepared by the core-shell method. The cores were produced by alkaline precipitation of iron oxide under high pressure homogenization conditions [1]. The BNF-Starch particles with different diameters were synthesized with the same iron oxide cores, but different coating conditions. The coating of the smaller BNF-Starch particles with hydroxyethyl starch was performed in water under high pressure homogenization conditions. The obtained particle suspension was fractionated at a permanent magnet. The supernatant was separated from the sediment to give the 80 nm BNF-Starch particles. The sediment was suspended in water to provide the 100 nm BNF-Starch particles. The coating of the larger BNF-Starch particles was carried out under sonication in a water bath. The obtained particle suspension was stored for 12 h at 4 °C. The supernatant was carefully removed with a pipette to give the 290 nm particles. The sediment was suspended in water to give the largest 350 nm BNF-Starch particles. An overview about the resulting particle sizes as well as particle size distributions is shown in Fig. 1 and Table 1.

Aqueous suspensions containing BNF particles of 80 nm, 100 nm, 290 nm and 350 nm in particle diameter were placed inside the cavity of Sepmag Q 100 ml. The schematic of the Sepmag device is shown in Fig. 2. The magnetic separation system is based on a cylindrical cavity within an arrangement of permanent hard magnets generating along to the radius a constant magnetic field gradient (14.1(1 ± 0.05) T/m) which is pointing towards the walls of the cavity (Sepmag Technologies, www.sepmag.eu). The inner diameter of the cavity is 62 mm and the bottle placed inside the cavity has the same outer diameter and a wall thickness of 2 mm. Therefore in the center of the cavity, the magnetic field strength is approximately 0 mT and at the inner side of the bottle's wall the maximal field strength should be $\mu_0 H$=409(1 ± 0.05) mT. It has to be considered that the gradient is constant over almost the whole area but at close proximity to the walls the actual magnetic field can be

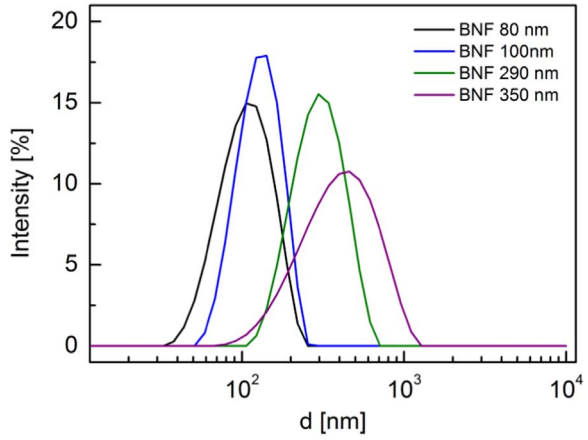

Fig. 1. Intensity weighted distribution of the hydrodynamic diameter for all investigated nanoparticles determined by DLS.

Table 1
Overview about Z-average diameters d and poly-dispersity index PDI for the investigated BNF nanoparticles.

Particle	BNF 80 nm	BNF 100 nm	BNF 290 nm	BNF 350 nm
d [nm]	98.4	121.0	289.7	343.6
PDI	0.085	0.077	0.178	0.189

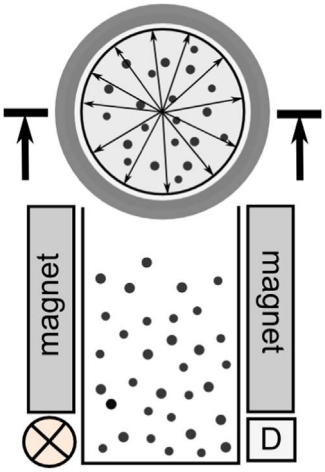

Fig. 2. Schematic drawing of the Sepmag device. Showing the magnets, light source (⊗) and detector (D).

higher due to the transition to the permanent magnet pieces used to build the system. The experiments were performed by placing a glass bottle containing 100 ml of aqueous suspension inside the cavity. Over time the opaque suspension becomes transparent. The glass bottle inside of the magnet is illuminated from one side of the cavity. On the other side a detector enables to monitor the magnetophoresis process.

The turbidity, T, of the separation process can be described by the equation:

$$T = T_\infty + \frac{T_0 - T_\infty}{1 + \left(\frac{t}{t_{50}}\right)^p}, \quad (1)$$

where T_0 is the initial turbidity, T_∞ the turbidity of the completely cleared solution, and t_{50} and p the separation parameters describing the actual separation process. t_{50} is the half separation time. Assuming non-cooperative magnetophoresis and particles of a single size the separation process should be described assuming p=2 [9]. Considering a real system of nanoparticles with a particle size distribution $p \neq 2$.

Furthermore, the iron content and the particle size distribution of the initial colloid, the sediment and the supernatant were monitored. The iron concentration was determined by colorimetric method. It is worth to mention that the iron concentration is directly proportional to the particle concentration. The hydrodynamic diameter (here Z-average) and the size distributions were determined by dynamic light scattering (DLS) using the Zetasizer Nano-ZS90 (Malvern Instr. Ltd.).

3. Results and discussion

For BNF nanoparticles at iron concentrations c > 0.10 mg(Fe)/ml the solution has such a high turbidity that the detector is already at its limit of sensitivity. Therefore information of turbidity changes during the initial phase of the separation process could be lost. For iron concentrations in the regime c≤0.01 mg(Fe)/ml the concentration is too low to modify the transmitted light significantly. Iron concentrations of 0.03 mg(Fe)/ml, mg(Fe)/ml and 0.10 mg(Fe)/ml were chosen to analytically study the separation processes of the particles. The separation processes for the three different iron concentrations are

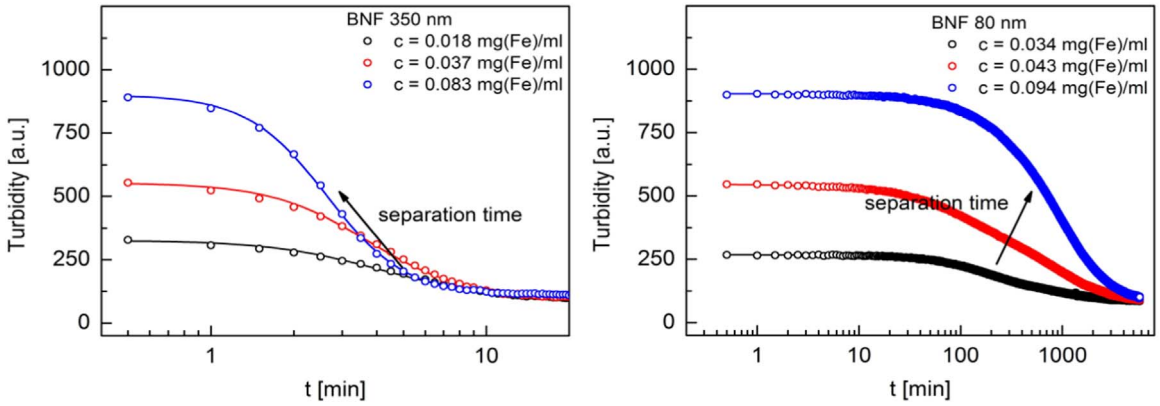

Fig. 3. Turbidity versus time of the separation processes for BNF 350 nm (left) and BNF 80 nm (right) particles for different initial iron concentrations of the suspension. The figures show the turbidity in dependence of time measured with the Sepmag system.

exemplarily shown for the BNF 80 nm and the BNF 350 nm particles in Fig. 3.

The nanoparticles were separated completely from the suspension for all investigated particle types and all three concentrations. Nevertheless the separation time varies by several orders of magnitude for the particle sizes changing from approximately 1000 min for the BNF 80 nm particles to below 10 min for the BNF 350 nm particles. For large nanoparticles, as for the BNF 350 nm particles shown in Fig. 3 (left), an increasing particle concentration led to a decrease in the separation time. Fig. 3 (right) shows the separation processes for the BNF 80 nm particles. The arrows in Fig. 3 indicate the change of the separation time for increasing iron concentration. Here, in comparison to the 350 nm particles an increase in the separation time with increasing iron concentration was observed.

For particle concentrations larger than 0.10 mg(Fe)/ml the sensitivity of the detector is too low for BNF particle. To investigate the overall separation process, 1 ml samples of the suspension were carefully taken at different times (0 h, 1 h, 16 h, 48 h and 112 h) at two different positions M1 and M2. The position M1 was 1 cm and M2 2 cm away from the wall of the bottle with 6 cm diameter. The investigated initial iron concentrations were 0.1 mg(Fe)/ml, 1.0 mg(Fe)/ml and 10.0 mg(Fe)/ml. Fig. 4 shows the observed separation processes. Fig. 4(left) shows exemplarily the separation process for an initial iron concentration of 10.0 mg(Fe)/ml at the two different positions M1 and M2. Fig. 4(right) presents the mean value of the normalized iron concentration for all three concentrations.

It was shown that the separation processes for the positions M1 and M2 are not significantly different. Nevertheless, for all separation processes investigated a slightly smaller iron concentration was observed for the position M2 closer to the middle of the bottle. Since the iron concentration did not differ significantly in the two points, the mean value of both was taken to compare the processes for different initial iron concentrations. Fig. 4 (right) shows this comparison as the normalized mean value of the iron concentration in dependence on time. For all three cases the separation processes also do not differ significantly from one another.

Differences in the behavior of the separation time in dependence on the initial particle concentration were found for different particle sizes. For the BNF 80 nm and the BNF 100 nm particles the separations time increases while for the BNF 290 nm and the BNF 350 nm particles the separation time decreases when the particle concentration increases. This is shown in Fig. 5. The vertical lines in the plot indicate the upper and lower limit for the detector implemented in the Sepmag Q for observing the whole separation process. The behavior for the BNF 290 nm and the BNF 350 nm particles is typical for separation processes of magnetic nanoparticles. With an increasing amount of particles in the suspensions the probability for chain formation increases and reduces the separation time [9]. To our knowledge, the slowdown of the separation process with rising iron concentration for smaller magnetic nanoparticles has not yet been reported.

The investigated BNF particles are stabilized by a dextran shell and show nearly identical Zeta-potential. Therefore all particles should show the same agglomeration behavior. Nevertheless, the diffusion coefficients can be concentration dependent as well as size dependent [16,17], both influencing the overall separation process. Furthermore, this behavior can be originated by a chain formation of larger nanoparticles due to dipole-dipole interactions. Particles of larger size preferably should form chains with one another and leave smaller

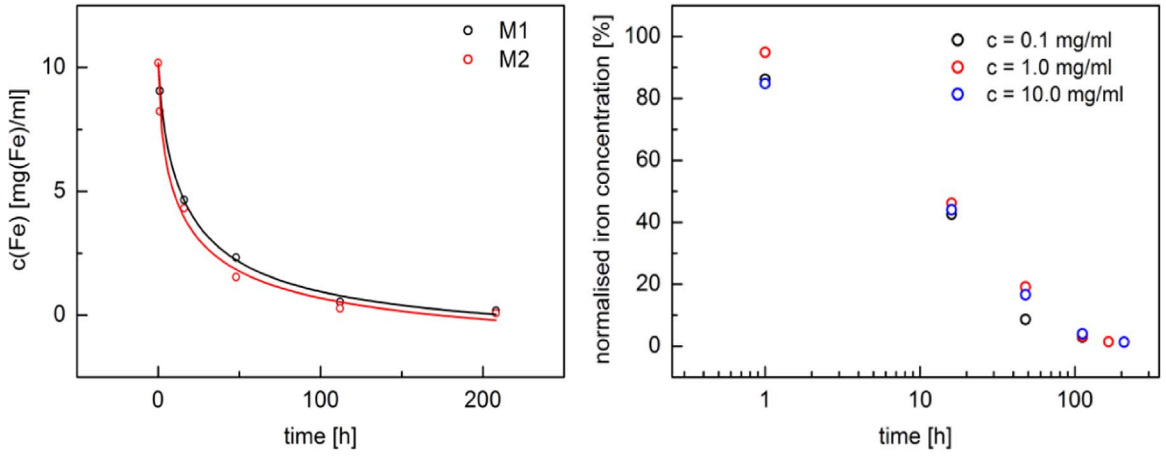

Fig. 4. Separation processes for BNF 80 nm particles for different initial iron concentrations of the suspension. The figures show the iron concentration in dependence of time for two different positions of extraction (left) and the mean value of the normalized iron concentration (right).

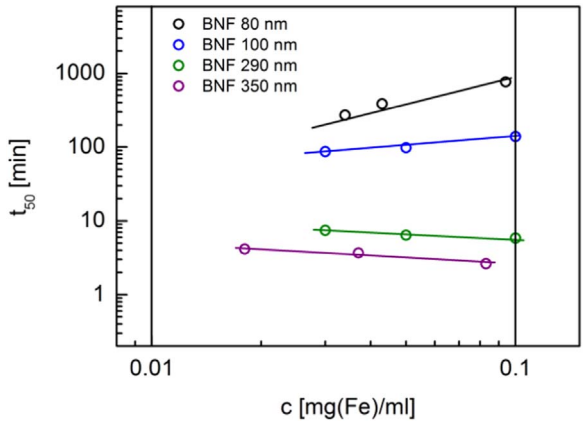

Fig. 5. Half separation time in dependence of the initial iron concentration for all investigated nanoparticles.

particles in the suspension. In general magnetic nanoparticles do not only show Brownian relaxation [18] but also Néel relaxation [19]. Particle behavior according to the Stoner-Wohlfarth model is assumed [20] instead of a magnetic multicore nanoparticle with a magnetic moment growing with increasing field strength. Each particle is characterized by a constant effective magnetic moment. This magnetic moment is oriented along the easy axis of magnetization assuming a uniaxial anisotropy. Depending on the size of the particles and the external magnetic field the magnetic moment can overcome the energy barrier separating the two energetic minima and flip the orientation.

Since the investigated dispersed particles are thermally blocked, i.e. Brownian relaxation is faster compared to the Néel relaxation they undergo Brownian relaxation. When a particle starts to move in the field gradient, probably Brownian relaxation will dominate, partially orienting the effective particle magnetic moment in the direction of the external field. When the particle moves into the direction of the wall in the Sepmag system the magnetic field rises. Therefore, the two energetic minima of the effective anisotropy become asymmetric in the field. Nevertheless, there is a probability that an isolated particle can flip the orientation of magnetization and slows down the separation process. When the particle concentration is increasing chains between particles are formed. If particles in the chain flip their orientation of magnetization, the dipole-dipole interaction can resuspend the particles. This could lead to a further slowdown of the separation process and hinder a stable chain formation.

For higher particle concentrations no significant change in the separation time of the BNF 80 nm particles could be observed, as shown in Fig. 6(left). This behavior was expected for non-cooperative magnetophoresis. The separation time does not change significantly by

Table 2
Mean hydrodynamic diameter, d, of BNF 80 nm particles in the supernatant after 16 h for different initial iron concentrations c.

c [mg(Fe)/ml]	0.1	1.0	10.0
d [nm]	96.7	92.3	90.2

increasing the particle concentration in the suspensions, but a systematic decrease in the hydrodynamic size of particles in the supernatant was observed for all cases. This was demonstrated by DLS measurements on the extracted samples (Fig. 6 right).

At higher particle concentration the mean particle diameter in the suspension decreases. This means that the larger particles in the size distribution move faster towards the wall of the bottle leaving smaller particles in the supernatant. This supports the assumption that larger nanoparticles in the suspension have a higher probability to interact because of the larger magnetic moment and form chains due to the lower interparticle distance at higher concentration which allows a higher rate of particle interaction. It leads to a faster separation from the liquid of larger particles. Taking this into account for the case of the BNF 80 nm particles the separation time is approximately 16 h. The derived mean values for the hydrodynamic diameter of particles in the supernatant are listed in Table 2.

Increasing the iron concentration leads to a decrease of the hydrodynamic diameter of initially 98.4 nm down to 90.2 nm for 10 mg(Fe)/ml. Taking into account a yield of 50%, smaller particles can be separated with a higher initial iron concentration.

If the particle concentration increases, the dipole-dipole interactions between nanoparticles become stronger. While smaller particles in the suspension still can change their magnetization orientation, larger particles will have a fixed magnetization parallel to the external magnetic field. Larger nanoparticles must overcome a larger energy barrier of the effective anisotropy. With increasing dipole-dipole interactions, this could lead to a stable chain formation for larger particles in the suspension, resulting in a cooperative separation. Smaller particles would still stay in the supernatant not showing cooperative behavior.

4. Conclusions

For large nanoparticles, i.e. BNF 290 nm and BNF 350 nm a reduction of the separation time was observed as expected for cooperative magnetophoresis when increasing the particle concentration. While for smaller nanoparticles, i.e. BNF 80 nm and BNF 100 nm a significant increase of the separation time was observed in the Sepmag Q 100 ml. For higher iron concentrations the separation time of the BNF 80 nm was approximately constant. The origin of this

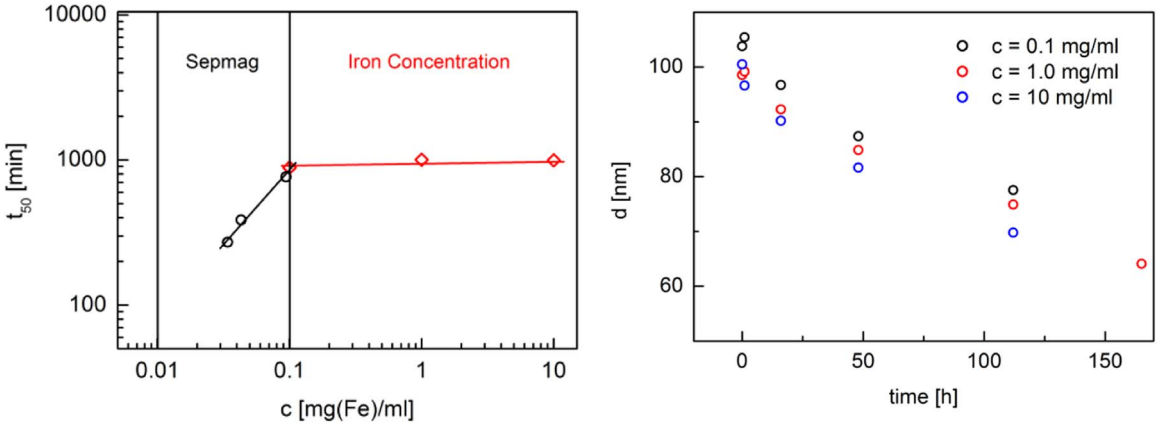

Fig. 6. Half separation time in dependence of the iron concentrations (left) and hydrodynamic particle diameter in the supernatant in dependence of time for different iron concentrations (right) for the BNF 80 nm particles.

increase in the separation time can be related to different effects which will be further studied. The increase in the separation time for BNF 80 nm and BNF 100 nm particles with rising iron concentration can be explained by a constant magnetic moment with two possible orientations along the easy-axis. The probability of flipping orientation may resuspend the particles and hinder a stable chain formation for small nanoparticles.

With increasing initial particle concentration in the suspension of these nanoparticles a decrease in the hydrodynamic diameter in the supernatant was observed. Taking into account the supernatant at the half separation time, a high yield with decreasing hydrodynamic size of particles can be obtained. These findings could be used and are promising for the further usage of the magnetic separation for the preparative fractionation of smaller magnetic nanoparticles at higher particle concentrations.

Acknowledgement

Financial support by European Commission Framework Programme 7 under NanoMag Project (grant agreement no. 604448) is acknowledged. We also would like to acknowledge the support of Dr. Lluis Martinez.

References

[1] C. Grüttner, et al., Synthesis and antibody conjugation of magnetic nanoparticles with improved specific power absorption rates for alternating magnetic field cancer therapy, J. Magn. Magn. Mater. 311 (1) (2007) 181–186.
[2] C. Grüttner, et al., Synthesis and functionalisation of magnetic nanoparticles for hyperthermia applications, Int. J. Hyperth. 29 (8) (2013) 777–789.
[3] R.S. Bejhed, et al., Turn-on optomagnetic bacterial DNA sequence detection using volume-amplified magnetic nanobeads, Biosens. Bioelectron. 66 (2015) 405–411.
[4] B. Zheng, et al. Quantitative stem cell imaging with magnetic particle imaging, in: 2013 International Workshop on Magnetic Particle Imaging (IWMPI), IEEE, 2013.
[5] A. Kasten, et al., Comparative in vitro study on magnetic iron oxide nanoparticles for MRI tracking of adipose tissue-derived progenitor cells, PloS One 9 (9) (2014) e108055.
[6] Q. Pankhurst, et al., Progress in applications of magnetic nanoparticles in biomedicine, J. Phys. D: Appl. Phys. 42 (22) (2009) 224001.
[7] V. Schaller, et al., Motion of nanometer sized magnetic particles in a magnetic field gradient, J. Appl. Phys. 104 (9) (2008) 093918.
[8] T. Rheinländer, et al., Magnetic fractionation of magnetic fluids, J. Magn. Magn. Mater. 219 (2) (2000) 219–228.
[9] J.S. Andreu, et al., Simple analytical model for the magnetophoretic separation of superparamagnetic dispersions in a uniform magnetic gradient, Phys. Rev. E 84 (2) (2011).
[10] M. Benelmekki, et al., Magnetophoresis behaviour at low gradient magnetic field and size control of nickel single core nanobeads, J. Magn. Magn. Mater. 323 (15) (2011) 1945–1949.
[11] M. Benelmekki, L.M. Martinez, Magnetophoresis of iron oxide nanoparticles: a tool for synthesis monitoring and biomagnetic applications, in: J.N. Govil, Naveen Kumar Navani, Shishir Sinha (Eds.), , Nanotechnology: Diagnostics and Therapeutics 7, Studium Press LLC / Researchco Books & Periodicals Pvt. Ltd., Houston, Texas, 2013, pp. 321–336 ISBN 10: 1626990077; ISBN 13: 9781626990074.
[12] M. Benelmekki, et al., Horizontal low gradient magnetophoresis behaviour of iron oxide nanoclusters at the different steps of the synthesis route, J. Nanopart. Res. 13 (8) (2011) 3199–3206.
[13] De. Las Cuevas, G.J. Faraudo, J. Camacho, Low-gradient magnetophoresis through field-induced reversible aggregation, J. Phys. Chem. C 112 (4) (2008) 945–950.
[14] F. Ludwig, et al., Magnetic, structural, and particle size analysis of single-and multi-core magnetic nanoparticles, IEEE Trans. Magn. 50 (11) (2014) 1–4.
[15] D.E. Bordelon, et al., Magnetic nanoparticle heating efficiency reveals magneto-structural differences when characterized with wide ranging and high amplitude alternating magnetic fields, J. Appl. Phys. 109 (12) (2011) 124904.
[16] S. Kutuzov, et al., On the kinetics of nanoparticle self-assembly at liquid/liquid interfaces, Phys. Chem. Chem. Phys. 9 (48) (2007) 6351–6358.
[17] C. Beenakker, P. Mazur, Diffusion of spheres in a concentrated suspension II, Phys. A: Stat. Mech. Appl. 126 (3) (1984) 349–370.
[18] J.I. Frenkel, Kinetic Theory of Liquids, Dover Publications, New York, 1955.
[19] L. Néel, Influence des fluctuations thermiques sur l'aimantation de grains ferromagnetiques tres fins, C.R. Hebd. Séances l'Acad. 228 (8) (1949) 664–666.
[20] E.C. Stoner, E. Wohlfarth, A mechanism of magnetic hysteresis in heterogeneous alloys, Philos. Trans. R. Soc. Lond. A: Math. Phys. Eng. Sci. 240 (826) (1948) 599–642.